# A DECONVOLUTION ALGORITHM FOR ESTIMATING JOINTLY THE LINE-OF-SIGHT CODE DELAY AND CARRIER PHASE OF GNSS SIGNALS

*Danai Skournetou*[1], *Ali H. Sayed*[2] *and Elena Simona Lohan*[1]

[1]Department of Communications Engineering, Tampere University of Technology
P.O.Box 553, FIN-33101, Finland;
{danai.skournetou, elena-simona.lohan}@tut.fi
[2]Department of Electrical Engineering, University of California,
Los Angeles, CA 90095, U.S.
sayed@ee.ucla.edu

## ABSTRACT

An important task of a Global Navigation Satellite System (GNSS) receiver is to achieve fine synchronization between the received Line-of-Sight (LOS) signal and the reference code, which would allow the computation of the satellite-receiver distance. This synchronization process, known also as tracking stage, requires the Doppler shift to be successfully removed from the received signal (or that the residual error is kept within allowable limits) and typically involves the estimation of signal parameters such as the code delay, the carrier frequency and/or carrier phase.

A challenging issue in the estimation of the synchronization parameters is the mitigation of multipath effects that appear due to the wireless propagation channel characteristics. In this paper, we deal with the problem of joint LOS code delay and carrier phase estimation of GNSS signals in a multipath environment. The problem is formulated into a linear system of equations in which the unknowns are the channel complex coefficients corresponding to each observed signal sample. We introduce a modified Projection Onto Convex Sets (POCS) algorithm that we optimize for both the new L1 Open Service and Coarse/Acquisition (C/A) signals employed by the future European Galileo and the Global Position System (GPS), respectively. We compare the performance of the algorithm with other state-of-art deconvolution algorithms. The simulation results indicate that our modified POCS algorithm is the most resistant in closely-spaced multipath static channels both when LOS code delay and carrier phase estimation are concerned.

## BIOGRAPHIES

**Danai Skournetou** received the M.Sc. degree in Information Technology from Tampere University of Technology in 2007. Currently, she is a PhD student in the Dept. of Communications Engineering of TUT where she also works as a researcher in the Digital Transmission Group (http://www.cs.tut.fi/~simona/Positioning Group Webpage.htm).

**Ali H. Sayed** is Professor and Chairman of Electrical Engineering at the University of California, Los Angeles. He is also the Principal Investigator of the UCLA Adaptive Systems Laboratory (www.ee.ucla.edu/asl).

**Elena Simona Lohan** is an Adjunct Professor at Tampere University of Technology, where she got her PhD degree in 2003. Her research interests include satellite positioning techniques, CDMA signal processing, and wireless channel modeling and estimation.

## I. INTRODUCTION

Knowledge of the Line-of-Sight (LOS) carrier phase is of great value in the context of Global Navigation Satellite Systems (GNSSs). Carrier-phase-based positioning is a representative example wherein phase information is fully utilized for pseudorange calculation at a sub-centimeter level [1]. Phase acquisition is also required for smoothing the ranging code measurements; it is normally performed in differential approaches and results in improved accuracy. Moreover, carrier phase estimation loops can be incorporated in the receivers for aiding the code tracking loops and improving their overall performance.

Although accurate carrier phase estimates are desirable, the presence of multiple channel paths causes distortions to the received signal, which cannot be treated via differential approaches due to the very localized nature of multipath [2]. Moreover, the characterization of the carrier phase multipath from field data is a difficult problem since the exact sources of these errors are not easily recognizable. In [3], the above-mentioned problem is approached from a geometric perspective that involves different configurations of the antenna-reflector(s) geometry. Carrier phase multipath is also commonly studied using a phasor diagram that illustrates the relation between the phase of the LOS signal and the multipath [4]–[6].

One can find in the literature other methods that aim to estimate carrier phase offsets assuming multipath environment. Such methods include the Ashtech Enhanced Strobe Correlator [7] and the Multipath Estimating Delay Lock Loop (MEDLL); the latter jointly estimates the delay, relative amplitude, and phase parameters of the multipath signals based on the maximum likelihood theory [8]. Both are advanced techniques with improved performance in long delay multipath errors, however, they are heavily patented.

A new modulation technique, called Binary Offset Carrier (BOC), has been introduced for future GNSS signals, including several Galileo signals as well as the GPS L5 signal [9]. Compared to the Binary Phase Shift Keying (BPSK) modulation used in GPS, with only one triangular-shaped peak in the envelope of the AutoCorrelation Function (Acf) (if unlimited bandwidth is assumed), BOC modulation introduces more challenges, both in the code delay and carrier phase tracking stages, due to the presence of multiple peaks (e.g., the possibility to track a wrong peak is higher). While the majority of the existing research work is done for GPS signals, only few studies can be found for the modernized GPS and new Galileo signals. In [10] the ability to track the phase of the GPS L5 signal in the presence of Gaussian noise was studied (both pilot and data channels were considered). Also, in [11] the performance of different phase discriminators was tested for the phase tracking of dataless channels, which have been included in the new BOC modulated signals. However, the ability to track the LOS phase of these new signal types in multipath environment is still to be investigated.

In this paper, we deal with the problem of joint LOS and carrier phase estimation in multipath environments, for BOC-modulated signals, by trying to overcome some of the above-mentioned limitations (namely, scarcity of methods able to estimate jointly phase and delay of LOS in multipath channels, limitation of most existing methods in the presence of multiple correlation peaks as in BOC modulation, high complexity of Maximum Likelihood-based algorithms).

We first formulate the multipath estimation problem in terms of a linear system of equations, where the unknowns are the channel complex coefficients corresponding to each observed signal sample. Then we apply deconvolution methods to solve this system and to find the correct code delay of each multipath component. The output is further used to form the carrier estimates. We also introduce a modified Projection Onto Convex Sets algorithm (i.e., a constrained deconvolution approach previously used for various CDMA systems [12]–[16]), which we optimize for both the new L1 Open Service and GPS signals.

Deconvolution approaches for LOS estimation have been previously used in [12], [17]. Our POCS-based proposed algorithm is different from the previously proposed deconvolution approaches in two main ways: first, it incorporates some knowledge about the static multipath channel via estimated level crossing rates of receiver correlation function; second, it uses an adaptive threshold to reduce the various sources of interference (noise, multipath, sidelobes in the autocorrelation function of BOC-modulated signals).

The remainder of this manuscript is organized as follows. Section II introduces the signal and the channel model. Section III includes the formulation of the problem whereas Section IV contains state-of-art methods, a step-by-step description of the modified POCS algorithm and how the LOS code delay and carrier phase are computed. Section V includes the simulation results and a discussion on the performance of the algorithms in various multipath channel profiles. Lastly, Section VI concludes the highlights of this research work and describes future plans.

## II. SIGNAL MODEL

The signals of interest are GPS and Galileo civil signals. Both use a Direct-Sequence Code Division Multiple Access (DS-CDMA) technique, and either BPSK for C/A code of GPS, or sine Binary-Offset-Carrier (BOC) modulation, for Galileo Open Services

(OS) [1], [18]. We notice that recent standardization documents specify Multiplexed BOC (MBOC) as the modulation type to be employed for OS signals and which is a combination of sine-BOC$(1,1)$ and sine-BOC$(6,1)$ [19]. However, since both BOC and MBOC modulation types have been incorporated in the standards, and since MBOC signals are supposed also to work with sine-BOC receivers, the focus here is on sine-BOC, and our algorithm requires only few (and straightforward) modifications to work with MBOC as well.

Therefore, the signal to be transmitted, $x(t)$, can be written as the convolution between the modulating waveform $s_{BOC}(t)$, the PseudoRaNdom (PRN) CDMA code and the modulated data, [20]:

$$x(t) = s_{BOC}(t) \star \sum_{n=-\infty}^{+\infty} \sum_{k=1}^{S_F} b_n c_{k,n} \delta(t - nT - kT_c) \tag{1}$$

where $\star$ is the convolution operator, $b_n$ is the $n$-th complex data symbol (in case of a pilot channel, it is equal to 1), $T$ is the symbol period, $c_{k,n}$ is the $k-$th chip corresponding to the $n-$th symbol, $T_c$ is the chip period, $S_F$ is the spreading factor ($S_F = T_{sym}/T_c$) and $\delta(t)$ is the Dirac pulse. The signal $s_{BOC}(t)$ stands for both BPSK and sine-BOC modulated signals, and it can be expressed as in Eq. (2) [20] (for cosine-BOC modulation, the expression of $s_{BOC}(t)$ is also given in [20]):

$$\begin{aligned} s_{BOC}(t) &= \pm \left( \sin \left( \frac{N_B \pi t}{T_c} \right) \right), \ 0 \le t \le T_c \\ &= p_{T_B}(t) \star \sum_{i=0}^{N_B - 1} (-1)^i \delta(t - iT_B) \end{aligned} \tag{2}$$

where $p_{T_B}(t)$ is the pulse shaping filter applied to pulses of duration $T_B = T_c/N_B$. For instance, if infinite bandwidth is assumed, $p_{T_B}(t)$ will be a rectangular pulse of unit amplitude if $0 \le t \le T_B$ and 0 otherwise. Here, $N_B$ is a modulation-related parameter, also called the BOC-modulation order [20]. For example, for the most encountered GNSS modulations, namely BPSK and sine-BOC(1,1) modulations, we have $N_B = 1$ and $N_B = 2$, respectively. For instance, if infinite bandwidth is assumed, $p_{T_B}(t)$ will be a rectangular pulse of unit amplitude if $0 \le t \le T_B$ and 0 otherwise. Here, $N_B$ is a modulation-related parameter, also called the BOC-modulation order [20]. For example, for the most encountered GNSS modulations, namely BPSK and sine-BOC(1,1) modulations, we have $N_B = 1$ and $N_B = 2$, respectively. An example of how a PRN waveform is modulated via sine-BOC$(1,1)$ (i.e. the signal $s_{BOC}(t)$ for $N_B = 2$) is shown in Fig. 1.

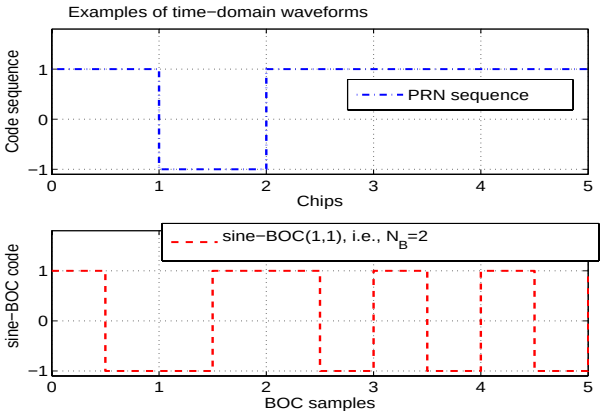


**Fig. 1**. Example of sine-BOC$(1,1)$ modulation.

Then, the signal $x(t)$ is modulated onto the carrier frequency $f_c$ and its passband form is given by

$$g(t) = \sqrt{E_b} \Re \Big\{ x(t) e^{-j2\pi f_c t} \Big\}, \tag{3}$$

where $E_b$ is the data bit energy and $\Re\{\cdot\}$ represents the real part. The signal $g(t)$ is typically transmitted over a multipath static or multipath fading channel where all interference sources (except for the multipaths) are lumped into a single additive Gaussian noise term $v(t)$:

$$r_x(t) = \sum_{l=1}^{L} \alpha_l \Re \Big\{ g(t - \tau_l) e^{-j(2\pi f_D t + \phi_l)} \Big\} + v(t), \tag{4}$$

where $r_x(t)$ is the received signal, $\alpha_l$, $\tau_l$ and $\phi_l$ are the amplitude, the code delay and the phase offset of the $l$-th path, respectively, $L$ is the number of channel paths, $f_D$ is the Doppler shift introduced by the channel, and $v(t)$ is the additive Gaussian noise of zero mean and double-sided power spectral density $N_0$.

The received signal $r_x(t)$ is then down-converted to a low IF frequency or to baseband using a conventional I/Q demodulator, followed by low-pass filtering for rejecting the higher frequency components. In our paper, we assume without loss of generality that the signal has been down-converted to baseband (the IF frequency can be then modeled as an additional Doppler shift). The baseband signal, $r_B(t)$, is now the

combination of the filtered in-phase (I) and quadrature (Q) demodulator branches:

$$\begin{aligned} r_B(t) &= r_{IB}(t) + jr_{QB}(t) + v_{I,Q}(t) \\ &= \sqrt{E_b}\sum_{l=1}^{L}\alpha_l x(t-\tau_l)[\cos(2\pi f_D t+\phi_l) \\ &\quad + j\sin(2\pi f_D t+\phi_l)] + v_{I,Q}(t) \\ &= \sqrt{E_b}\sum_{l=1}^{L}\alpha_l x(t-\tau_l)e^{j(2\pi f_D t+\phi_l)} \\ &\quad + v_{I,Q}(t) \end{aligned} \quad (5)$$

where $f_D$ is the Doppler shift to be removed during the acquisition stage and the new noise term $v_{I,Q}(t)$ can be shown to have the same power as $v(t)$.

After the signal is acquired, fine code synchronization is required for successfully despreading the signal. Both acquisition and delay tracking stages (i.e., code synchronization) are usually based on the code epoch correlation between the incoming down-converted signal and the reference modulated PRN code ($x_{ref}$), with a certain candidate Doppler frequency $\widehat{f}_D$, delay $\widehat{\tau}$ and phase offset $\widehat{\phi}$ given by

$$\begin{aligned} x_{ref}(\widehat{\tau},\widehat{f}_D,\widehat{\phi}) &= \Bigg(s_{BOC}(t-\widehat{\tau}) \star \sum_{n=-\infty}^{+\infty}\sum_{k=1}^{S_F}\widehat{b}_n \\ &\quad \times c_{k,n}\delta(t-nT-kT_c-\widehat{\tau})\Bigg) \\ &\quad \times e^{j(2\pi\widehat{f}_D t+\widehat{\phi})} \end{aligned} \quad (6)$$

In order to generate $x_{ref}(\cdot)$ we first assume a certain Doppler shift estimate $\widehat{f}_D$ (produced in the acquisition stage), then the code delay ($\widehat{\tau}$) and the phase offset ($\widehat{\phi}$) of the LOS signal are estimated by cross-correlating $r_B(t)e^{-j(2\pi\widehat{f}_D t)}$ with $x(t-\tau_k)$ where $\tau_k$ belongs to a candidate region of delays. The cross-correlation function is given by

$$\mathcal{R}_m(\tau_k) = \mathbf{E}\left(\frac{1}{T}\int_{(m-1)T}^{mT} r(t)e^{-j2\pi\widehat{f}_D t}x(t-\tau_k)dt\right) \quad (7)$$

where $m$ is the code epoch index and $\mathbf{E}(\cdot)$ is the expectation operation, with respect to the PRN code. In order to reduce the noise level, both coherent ($\widetilde{\mathcal{R}}(\tau_k)$) and non-coherent ($\overline{\mathcal{R}}(\tau_k)$) integration may be used. The averaged coherent and non-coherent

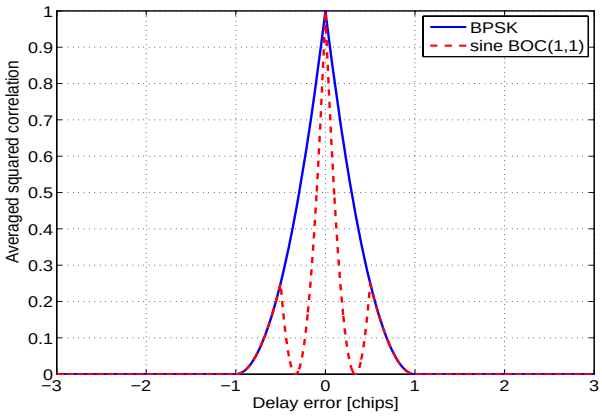


**Fig. 2**. Example of averaged squared correlation function with pulse shaping for BPSK and sine-BOC(1,1) modulation in single-path channel.

correlation function can be written as

$$\widetilde{\mathcal{R}}(\tau_k) = \frac{1}{N_c}\sum_{m=1}^{N_c}\mathcal{R}_m(\tau_k) \quad (8)$$

$$\overline{\mathcal{R}}(\tau_k) = \frac{1}{N_{nc}}\sum_{N_{nc}}\left|\widetilde{\mathcal{R}}(\tau_k)\right|^2 \quad (9)$$

where $N_c$ is the coherent integration time (expressed in code epochs or ms for GPS/Galileo signals) and $N_{nc}$ is the non-coherent integration time, expressed in blocks of length $N_c$ ms (note that the subscript $m$ has been dropped in Eqs. (8) and (9) for clarity reasons). Examples of the averaged squared correlation function for BPSK and sine-BOC(1,1) modulation for one- and two- path channel, no noise, zero residual Doppler error, no phase offset and unit bit energy are shown in Fig. 2.

## III. PROBLEM FORMULATION

The target is to estimate jointly the code delay and the carrier phase offset of the LOS signal. If we substitute $r_B(t)$ into Eq. (7), after some manipulations, we can write the output of the crosscorrelation function $y_R$ as

$$y_R = \sqrt{E_b}\sum_{l=1}^{L}\alpha_l R_m(\tau_i,\tau_j)e^{-j(2\pi\Delta_{f_D}t+\phi_l)} + v(t), \quad (10)$$

where $\Delta_{f_D}$ is a small residual error that is equal to $\widehat{f}_D - f_D$ and resulted from the Doppler estimation during the acquisition stage and $R_m(\tau_i,\tau_j)$ is the

ideal auto-correlation function of the modulated code given by

$$R_m(\tau_i,\tau_j)=\mathbf{E}\left(\frac{1}{T}\int_{(m-1)T}^{mT}x(t-\tau_i)x(t-\tau_j)\right), \quad (11)$$

where $\tau_i$,$\tau_j$ belong in the range of possible code delays. It is possible to rewrite Eq. (10) into a system of linear equations [21]:

$$\begin{bmatrix} y_0 \\ \vdots \\ y_{d_{max}} \end{bmatrix} = \begin{bmatrix} h_{0,0} & \cdots & h_{0,d_{max}} \\ \vdots & \ddots & \vdots \\ h_{d_{max},0} & \cdots & h_{d_{max},d_{max}} \end{bmatrix} \begin{bmatrix} w_0 \\ \vdots \\ w_{d_{max}} \end{bmatrix} + \begin{bmatrix} v_0 \\ \vdots \\ v_{d_{max}} \end{bmatrix}, \quad (12)$$

where $y_i$ is the complex correlation output at code delay $\tau_i$ computed by Eq. (7) for $i=0$ till the maximum delay spread of the channel, $d_{max}=\tau_{max}T_s$, where $T_s$ is the sampling period. The $d_{max}\times d_{max}$ matrix $\mathbf{H}$ is the pulse shape deconvolution matrix, each element, $h_{i,j}$, of which is equal to $\sqrt{E_b}R_m(\tau_i,\tau_j)$ (note that $\mathbf{H}$ is a real Toeplitz matrix) and the vector $\underline{\mathbf{v}}$ contains the complex AWGN noise terms of the despreaded signal. The elements of the unknown vector $\underline{\mathbf{w}}$ have the following interpretation: ideally, if a path is present at delay $\tau_i$, then $w_i$ should be $a_i e^{j\phi_i}$, else $w_i=0$. Now, the target is to estimate the non-zero elements of $\underline{\mathbf{w}}$; the positions of which indicate the path delays. Thus, we have the problem of solving a linear system of equations, where the path positions, amplitudes and phases are changing in time. Moreover, the phase offsets can be computed by using an appropriate phase discriminator function. In the following section, we describe some methods that can be applied for solving the above-mentioned linear problem and for resolving the multiple paths.

## IV. MULTIPATH DECOMPOSITION

Now that we have formulated our problem into a system of linear equations, we can consider some methods for estimating the unknown vector $\underline{\mathbf{w}}$. Let us first write Eq. (12) into compact form as

$$\underline{\mathbf{y}}=\mathbf{H}\underline{\mathbf{w}}+\underline{\mathbf{v}} \quad (13)$$

One well-known approach for dealing with such linear models is to minimize the squared difference between the data (known vector $\underline{\mathbf{y}}$) and $\mathbf{H}\underline{\mathbf{w}}$. The solution of the so-called Least Squares (LS) problem is

$$\underline{\widehat{\mathbf{w}}}_{LS}=(\mathbf{H}^T\mathbf{H})^{-1}\mathbf{H}^T\underline{\mathbf{y}} \quad (14)$$

Another approach is to minimize the mean square error (MMSE) and its solution is given by

$$\underline{\widehat{\mathbf{w}}}_{MMSE}=\left(\widehat{\sigma}^2\mathbf{I}+\mathbf{H}^T\mathbf{H}\right)^{-1}\mathbf{H}^T\underline{\mathbf{y}}, \quad (15)$$

where $\widehat{\sigma}^2$ is the estimated noise variance and letter $T$ is used to denote matrix transposition.

A third approach, namely Projection Onto Convex Sets (POCS), is an iterative constrained deconvolution approach which was originally proposed in [14], [16] for delay estimation in Rake receivers. More precisely, POCS finds a solution that complies with a predefined set of constraints. Each constraint is used to form a closed convex set and the estimate that satisfies them all is the POCS solution. For example, an estimate for $\underline{\mathbf{w}}$ is found via

$$\underline{\widehat{\mathbf{w}}}_{POCS^*}=\mathcal{P}\underline{\mathbf{w}}, \quad (16)$$

where $\mathcal{P}$ is the operation of projecting the solution $\underline{\mathbf{w}}$, onto the convex set $\mathcal{C}$. When the constraint is applied on the variance of the estimation error (i.e., on the variance of $\underline{\mathbf{y}}-\underline{\widehat{\mathbf{w}}}_{POCS^*}$) then the convex set can be defined as [13], [14]

$$\mathcal{C}=\{\mathbf{f}:\|\underline{\mathbf{y}}-\mathbf{H}\mathbf{f}\|^2\leq\beta\}, \quad (17)$$

where $\beta$ is a scalar bound that is a function of the noise variance after integration. The traditional POCS solution at the $(k)$-th iteration can be written as [22]:

$$\underline{\widehat{\mathbf{w}}}_{POCS}^{(k)} = \underline{\widehat{\mathbf{w}}}_{POCS}^{(k-1)}+\left(\frac{1}{\lambda}\mathbf{I}+\mathbf{H}^T\mathbf{H}\right)^{-1}\mathbf{H}^T \times\left(\underline{\mathbf{y}}-\mathbf{H}\underline{\widehat{\mathbf{w}}}_{POCS}^{(k-1)}\right) \quad (18)$$

where $\lambda$ is the Lagrange multiplier associated with the variance of the residual constraint and $\mathbf{I}$ is the unity matrix. The optimal $\lambda$ is found when the noise variance is known or when it is a-priori estimated. Starting with an initial estimate, the algorithm converges to a feasible solution by cyclically projecting onto the constraint sets [13]. In [21], a modified POCS was used for path acquisition in WCDMA systems with promising results.

### IV-A. Proposed POCS

We now describe how POCS can be adjusted to fit our problem. As it was mentioned earlier, POCS utilizes a set of constraints with the aim of reducing the estimation error. The first constraint employed by POCS is the one related to the range of possible delays. In particular, in each iteration $k$, only the delay estimates that are located within a window of $\pm\gamma$ chips around the position of the estimate with the maximum magnitude are considered. The delay range constraint $\mathcal{P}_1$ is defined as

$$\mathcal{P}_1 : z_i = \begin{cases} z_i, & \text{if } i \in [\breve{\tau}-\gamma \quad \breve{\tau}+\gamma] \\ 0, & \text{else} \end{cases} \tag{19}$$

where $z_i$ is the $i$-th element of a vector $\underline{\mathbf{z}}$, $\gamma$ is a predefined constant (here it depends on the modulation index $N_B$) and $\breve{\tau}$ is given by

$$\breve{\tau} = \arg\max_{\tau} \underline{\mathbf{z}} \tag{20}$$

Imposing such a constraint ensures that POCS is applied on the area where most of the signal power is present under the assumption that the signal dominates noise. The second constraint, $\mathcal{P}_2$, has to do with the magnitude of the estimates. More precisely, we would like to keep only the estimates $z_i$ which are larger than a threshold $\xi$:

$$\mathcal{P}_2 : z_i = \begin{cases} z_i, & \text{if } z_i \geq \xi \\ 0, & \text{else} \end{cases} \tag{21}$$

We notice that $\mathcal{P}_1$ and $\mathcal{P}_2$ differ from the $\mathcal{P}$ constraint in that they are applied after the adaptation step has taken place, i.e., they are not used for forming the iterative POCS solution as it is done in the original POCS.

Now, we can describe the steps of the proposed algorithm. First, we see that POCS is applied for each non-coherent block separately and that for each non-coherent block we use $\underline{\mathbf{y}}^{(nc)}$ as the initial state for $\underline{\widehat{\mathbf{w}}}_{POCS}$, where $nc$ is the $nc$-th non-coherent block. Then for each iteration, the adaptation rule is applied. Notice that the constant term $1/\lambda$ which appears in the original form of POCS algorithm has been now substituted by the dynamically estimated noise variance. Another important element of the algorithm is the choice of the threshold $\xi$. Its computation is based on the Level Crossing Rate (LCR) of the normalized non-coherent $Acf$ and which is defined as the number of crossings (both from below and from above) at level $l_j$. Assuming that the time samples of the normalized correlation function $\overline{\mathcal{R}}(\tau_k)/\max(\overline{\mathcal{R}}(\tau_k))$ with $\overline{\mathcal{R}}(\tau_k)$ denoted in Eq. (9), are denoted by $\overline{\mathcal{R}}_k$ and that they are taken at sampling instants $\tau_k$, $k = 1, 2, \ldots$, then:ł

$$\begin{aligned} LCR(l_j) \quad = \quad & card\Big\{k|(\overline{\mathcal{R}}_k \leq l_j \wedge \overline{\mathcal{R}}_{k+1} > l_j) \\ & \bigwedge (\overline{\mathcal{R}}_{k+1} \leq l_j \wedge \overline{\mathcal{R}}_k > l_j)\Big\}, \end{aligned} \tag{22}$$

where $card$ is the cardinal of a set and $\wedge$ is 'and' operator. The potential of LCR information in GNSS context was noted in [23], where it was found that it can be used as a reliable indoor/outdoor CNR identifier. However, the LCR information can be also used within the code tracking context for thresholding the Acf [24]. Here, we also apply the LCR function on the normalized non-coherent $Acf$ in order to compute $\xi$; however, the threshold is applied on the vector $\underline{\widehat{\mathbf{w}}}_{norm}^{(k,nc)}$ at each iteration. The reason for using the LCR information to define the second POCS constraint is that we can discard the noisy estimates. More precisely, we have found that at lower levels, where the majority of noise "spikes" are present, the LCR is larger than in the higher Acf levels (e.g. above noise floor) [23], [24]. Consequently, the level that corresponds to the maximum LCR will reveal also the level in which $Acf$ is the most noisy and thus we can use it to reject the noisy estimates in $\underline{\widehat{\mathbf{w}}}_{POCS}^{(k,nc)}$. For brevity, we have omitted the more detailed description of the LCR concept; interested readers may refer

**Algorithm 1** POCS Algorithm for multipath decomposition

1. For $nc = 1$ to $N_{nc}$
   2. Set $\underline{\widehat{\mathbf{w}}}_{POCS}^{(0,nc)} = \underline{\mathbf{y}}^{(nc)}$
   3. For $k = 1$ to $K_{iter}$

$$\underline{\widehat{\mathbf{w}}}_{POCS}^{(k,nc)} = \underline{\widehat{\mathbf{w}}}_{POCS}^{(k-1,nc)} + \left(\widehat{\sigma}^2\mathbf{I} + \mathbf{H}^T\mathbf{H}\right)^{-1} \times \mathbf{H}^T\left(\underline{\mathbf{y}}^{(nc)} - \mathbf{H}\underline{\widehat{\mathbf{w}}}_{POCS}^{(k-1,nc)}\right)$$

$$\underline{\widehat{\mathbf{w}}}_{norm}^{(k,nc)} = |\underline{\widehat{\mathbf{w}}}_{POCS}^{(k,nc)}|^2 / \max\left(|\underline{\widehat{\mathbf{w}}}_{POCS}^{(k,nc)}|^2\right)$$

   4. Apply $\mathcal{P}_1$ and $\mathcal{P}_2$ constraints $\widehat{w}_{norm}^{(k,nc)}(i)$ of $\underline{\widehat{\mathbf{w}}}_{norm}^{(k,nc)}$
   5. If $\widehat{w}_{norm}^{(k,nc)} \neq 0$

$$\widehat{w}_{POCS}^{k,nc}(i) = \widehat{w}_{POCS}^{k,nc}(i)$$

   Else

$$\widehat{w}_{POCS}^{k,nc}(i) = 0$$

to [23], [24]. Given the Acf level $\breve{q}$ that results in maximum LCR, the POCS threshold is computed as

$$\xi = \min\left\{[\breve{q} + 0.5 \quad 0.99]\right\}, \quad \text{for } N_B = 1, 2 \quad (23)$$

$$\breve{q} = \arg\max_{q} LCR(q) \quad (24)$$

The constant of $0.5$ has not been added to $\breve{q}$ arbitrarily. In particular, we performed a set of simulations in which we tested the performance of POCS algorithm for different values, starting from $0.1$ and up to $0.8$ with a step of $0.1$ and we found the when we add $0.5$ to $\breve{q}$ we get the best performance. The results of our experiments are not included due to the limited space.

### IV-B. LOS delay and phase estimation

Here, we describe how the LOS signal is detected and also how the code delay and phase offset are computed. In all algorithms, we apply non-coherent integration on the returned complex vector $\widehat{\mathbf{w}}_{POCS}^{K_{iter},nc}$ in order to further reduce the noise. Then, the LOS signal, for both LS and MMSE, is the estimate with the maximum magnitude. The LOS code delay estimate for LS and MMSE algorithms are given by

$$\widehat{\tau}_{LS} = \arg\max_{\tau} \frac{1}{N_{nc}} \sum_{N_{nc}} \left|\underline{\widehat{\mathbf{w}}}_{LS}^{(K_{iter},nc)}\right|^2 \quad (25)$$

$$\widehat{\tau}_{MMSE} = \arg\max_{\tau} \frac{1}{N_{nc}} \sum_{N_{nc}} \left|\underline{\widehat{\mathbf{w}}}_{MMSE}^{(K_{iter},nc)}\right|^2 \quad (26)$$

Concerning the POCS algorithm, we tested two different cases. In the first case, the LOS signal is detected as in LS and MMSE (i.e., based on the maximum magnitude). In the second case, the LOS signal is the one that corresponds to the first estimate of the non-coherent estimated vector ($\underline{\widehat{\mathbf{w}}}_{POCS}^{new}$) that is above a threshold $\xi$. The estimated LOS delays for the first ($POCS1$) and second ($POCS2$) case are given by

$$\widehat{\tau}_{POCS1} = arg\max_{\tau} \frac{1}{N_{nc}} \sum_{N_{nc}} \left|\underline{\widehat{\mathbf{w}}}_{POCS}^{(K_{iter},nc)}\right|^2 \quad (27)$$

$$\widehat{\tau}_{POCS2} = \underline{\widehat{\mathbf{w}}}_{POCS}^{new}(1), \quad (28)$$

where $\underline{\widehat{\mathbf{w}}}_{POCS}^{new}$ is given by

$$\underline{\widehat{\mathbf{w}}}_{POCS}^{new} = \left\{ \widehat{w}_{POCS}^{K_{iter}}(i) : \frac{1}{N_{nc}} \sum_{N_{nc}} \left|\widehat{w}_{POCS}^{K_{iter},nc}(i)\right|^2 \geq \xi \right\} \quad (29)$$

After the LOS delay has been determined, the LOS phase offset for each algorithm ($\widehat{\phi}_{algo}$) is computed as

$$\widehat{\phi}_{algo} = \mathcal{F}^{-1}\left(\Re\{\underline{\widehat{\mathbf{w}}}_{algo}(\widehat{\tau}_{algo})\}, \Im\{\underline{\widehat{\mathbf{w}}}_{algo}(\widehat{\tau}_{algo})\}\right) \quad (30)$$

where $\mathcal{F}$ is a properly chosen phase discriminator function. When the data bits have been already removed or when we deal with dataless channels (e.g., Galileo OS signals), the inverse double arctan discriminator function ($\mathcal{F} = \tan_2^{-1}$) is the most appropriate due to its wide linear range of operation (i.e. it can detect phases that vary between $-\pi$ to $\pi$) and better noise resistance [10], [11], [25].

## V. SIMULATION RESULTS

The main target of the simulations is to compare the performance of the modified POCS algorithm (POCS1 and POCS2 versions) with the LS and MMSE methods. Regarding POCS algorithm, we empirically found via simulations that three iterations ($K_{iter} = 3$) were adequate for satisfactory performance, but we omit here the experimental results for the sake of clarity. Moreover, $\gamma$ was set to 2 chips when $N_B = 1$ and to 1 chip when $N_B = 1$. Moreover, the noise variance $\sigma^2$ utilized by MMSE and POCS was estimated from the non-coherent Acf by using first order statistics.

In addition, we have included two more cases for reference purposes. In the first one, the LOS code delay is simply estimated by the position of $\max(Acf)$ in the time axis and then the LOS phase is computed by applying the inverse double arctangent discriminator function on the coherent $Acf$ at the estimated LOS delay. In the second scenario, we would like to compare the estimators performance with the ideal code delay estimator, meaning when the estimated LOS delay is the true one and the LOS phase is computed using the same phase discriminator as in the rest of the algorithms (i.e. double arctan). Of course for the case of true delay the error is zero as expected, but we are also interested in looking at the estimated phase when it is computed (based on the coherent Acf as well) using the true delay.

We performed simulations for both sine-BOC$(1,1)$ and BPSK modulated signals. First, we give a detailed description of the channel profiles and simulation parameters we used. Second, we present the results and analyze the estimators performance in terms of Root Mean Square Error (RMSE).

### V-A. Simulation parameters

Regarding the channel setup, we considered only the case of static multipath channel because we wanted to see the maximum achievable performance, and because modeling the phases in fading channels introduces additional errors. More precisely, the model we used employs a decaying Power Delay Profile (PDP), meaning that $\overline{\alpha_l} = \overline{\alpha_1} e^{-\zeta_{PDP}(\tau_l - \tau_1)}$, where $\overline{\alpha_1}$ is the average amplitude of the 1-st path and $\zeta_{PDP}$ is the power decaying profile coefficient, (assumed in the simulations to be equal to $0.09$ when the path delays are expressed in samples).

The number of channel paths varied between $1$ and $4$, while the carrier phase offset introduced in the $l$-th was assumed to be uniformly distributed between $-\pi$ and $\pi$. The time separation between successive paths $\tau_{l+1,t} - \tau_{l,t}$, at any time instance $t$, was assumed to be uniformly distributed between $0$ and $0.35$ chips for BOC modulated signals or between $0$ and $1$ (i.e. between $0$ and half the width of the main lobe of the Acf). The latter parameter values indicate closely-spaced paths which are typical in indoor and densely populated urban scenarios. The oversampling factor was equal to $10$ for both BOC$(1,1)$ (i.e., the number of samples per BOC interval) and BPSK modulation. The processing of Acf is done in a window ($S$) of $8$ chips length with a resolution of $0.1$ and $0.05$ chips in the case of BPSK and BOC$(1,1)$ modulation, respectively (in BOC signals we need finer resolution due to the more complicated shape of Acf). The coherent integration time ($N_c$) was set to $20$ ms, while the non-coherent integration ($N_{nc}$) was performed in $2$ blocks of $N_c$ length. The simulations are based on $Nrand = 5000$ random realizations (of channel and signals), each realization having an observation interval of $N_c N_{nc}$ ms.

### V-B. Discussion

We start our discussion first on the results where BPSK-modulated signal is used and then when BOC modulation is used.

In the top of Fig. 3, we see the performance of the estimators in single-path profile. At lower CNR values ($30 - 35$ dBHz), the time delay that corresponds to $max(Acf)$ seems to best represent the LOS delay. POCS1, POCS2 and MMSE reach $RMSE = 0$ for $CNR \geq 35$ dBHz while LS seems to perform the worst. We note, that due to the logarithmic scale used for plotting, the curve for the RMSE of true delay, being $0$, is not visible. When LOS phase is concerned, the RMSE derived based on $\max(Acf)$ and LOS true delay are the same, POCS1 and POCS2 also perform similarly, and LS follows last (see bottom of Fig. 3).

One may wonder why, for example at $CNR = 30$ dBHz, when we estimate LOS delay based on $\max(Acf)$ we have $RMSE \approx 8$ meters but when we estimate the LOS phase at same CNR, RMSE is the same with the case where LOS phase is computed based on true delay. In order to get a better understanding on this observation, we can look at the top of Fig. 4 where an instance of the LOS absolute carrier phase error versus the code delay error is depicted for $CNR = 30$ dBHz. From the figure we notice that the phase error is not the minimum when the delay error is but it rather fluctuates around the zero delay error. We have also encountered similar behavior of the phase error at very high CNR values, thus the presence of the noise cannot fully explain the above mentioned situation. An in-depth research on the relation between the delay and carrier phase error is not in the scope of this paper and belongs to our future plans.

When the number of paths is increased to $2$, we see the overall performance of the estimators deteriorates as expected (see Fig. 5). However, now POCS2 has the best performance for $CNR \geq 40$ dBHz both for delay and phase estimation. Also, we see that although the RMSE of LOS phase decreases as CNR increases for LS, MMSE and POCS, it remains almost constant when the phase is estimated based on $\max(Acf)$ or on the true delay. This saturated behavior also implies the need for sophisticated algorithms even when the CNR conditions are very good. When we have $3$ or $4$ paths present, the performance of POCS2 remains the best for both phase and delay estimation (see Figs. 6 and 7). In particular, when CNR is very high (e.g. above $55$ dBHz) the RMSE for POCS2 reaches the zero level. We also notice, that when the number of paths is greater than $2$, looking at the delay that corresponds to $\max(Acf)$ leads to significant errors even at very good CNR conditions.

When BOC$(1,1)$ modulated signals are used, we see that in the single path scenario, there is some slight deterioration in the performance of the algorithms in respect to RMSE delay when compared with the case of BPSK modulation (see Fig. 8). When the number of paths is increased, we see that the performance of POCS2 is significantly better for middle to higher CNRs when compared to the rest

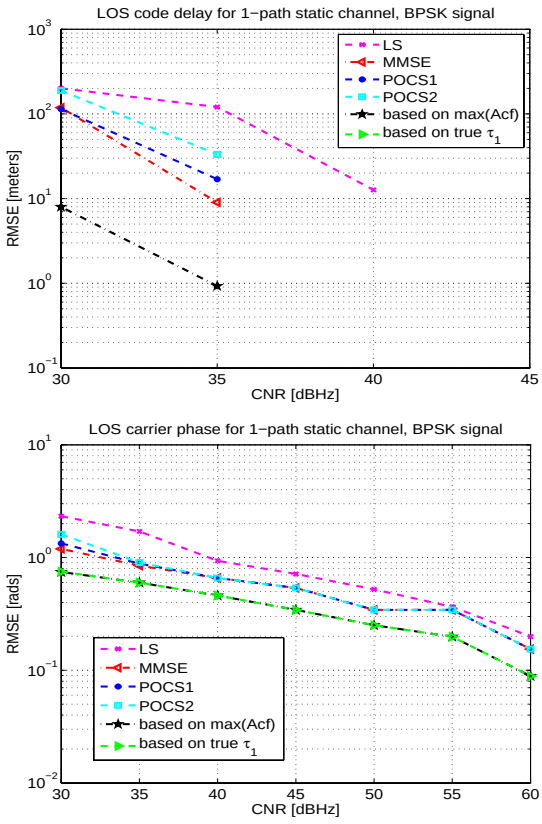


**Fig. 3**. RMSE of LOS code delay and carrier phase offset vs. CNR for 1-path static channel, BPSK modulation and infinite bandwidth.

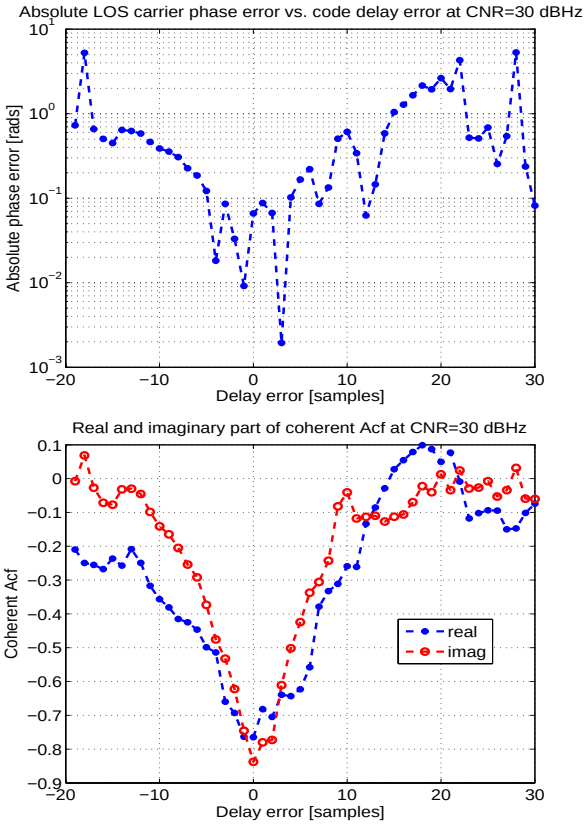


**Fig. 4**. Absolute LOS phase error vs. delay error (top). Real and imaginary parts of coherent Acf, for single path static channel at $CNR = 30$ dBHz.

and for both delay and phase estimation (see Figs. 9 and 10). We also notice that we have obtained similar results for a 4 path static channel but due to the limited space they are not included here.

## VI. CONCLUSIONS AND FUTURE WORK

In this paper, we proposed a modified POCS algorithm for estimating jointly the code delay and the carrier phase of the received LOS signal. The proposed algorithm has been optimized for both the new L1 Open Service and GPS signals and it is compared with other state-of-art methods (namely Least Square and Minimum Mean Square approaches) that are applicable in problems where multipath decomposition is required.

We tested the performance of the proposed algorithm in terms of Root Mean Square Error versus CNR for various multipath profiles and static channel. The results were based on Monte Carlo simulations and showed that the proposed alternation of POCS is the most resistant in closely-spaced path environments when good CNR conditions occur. In the case of single-path scenario, the proposed algorithm seems to be affected more by the noise when it is used for LOS carrier phase estimation. To overcome this limitation, our future plans include the incorporation of a mechanism that would allow to differentiate the algorithm depending on whether single or multipath channel is detected. In particular, the method described in [17] has been shown to have very good performance in terms of detection probability, therefore it is an excellent choice for further optimizing the proposed algorithm. Other future plans include the assessment of the modified POCS in the case where fading channel is assumed and when MBOC modulation is used.

## VII. ACKNOWLEDGMENTS

This work was carried out in the project ”Future GNSS Applications and Techniques (FUGAT)”

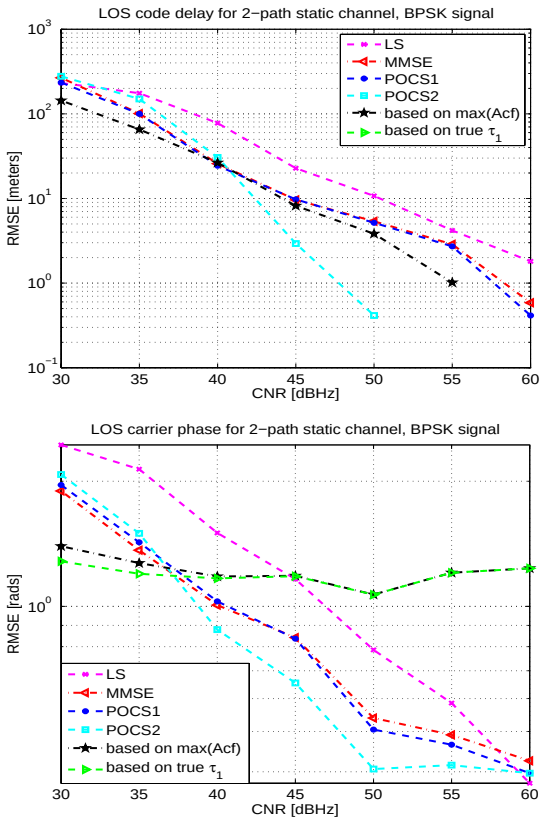


**Fig. 5**. RMSE of LOS code delay and carrier phase offset vs. CNR for 2-path static channel.

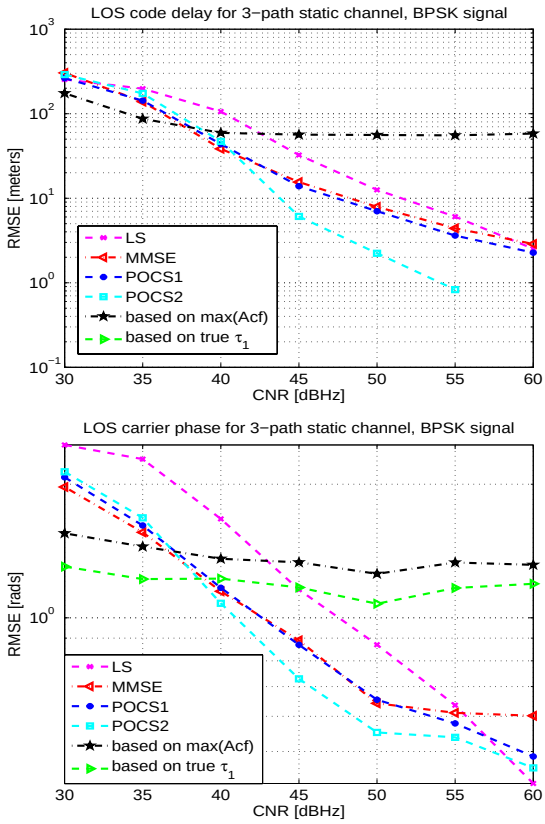


**Fig. 6**. RMSE of LOS code delay and carrier phase offset vs. CNR for 3-path static channel.

funded by the Finnish Funding Agency for Technology and Innovation (Tekes). The work of A. H. Sayed was supported in part by NSF grants ECS-0601266 and ECS-0725441.

## VIII. REFERENCES

[1] E. Kaplan, *Understanding GPS: Principles and Applications*. Artech House, 1996.

[2] M. Braasch, *Multipath Effects, Global Positioning Systems: Theory and Applications*. American Institute of Aeronautics and Astronautics, 1996, vol. 1, ch. 14, pp. 547-568.

[3] J. K. Ray and M. E. Cannon, "Characterization of GPS carrier phase multipath," in *ION NTM*, San Diego, California, January 1999, pp. 343–352.

[4] M. Braasch and A. van Dierendonck, "GPS receiver architectures and measurements," *IEEE*, vol. 87, no. 1, pp. 48–64, January 1999.

[5] S. K. Kalyanaraman and M. S. Braasch, "Influence of GPS code tracking on carrier phase multipath performance," *IEEE Aerospace Conference*, vol. 3, p. 1686, March 2004.

[6] S. K. Kalyanaraman, M. S. Braasch, and J. M. Kelly, "Code tracking architecture influence on GPS carrier multipath," *IEEE Transactions on Aerospace and Electronic Systems*, vol. 42, no. 2, pp. 548–561, 2006.

[7] L. Garin and J. Rousseau, "Enhanced strobe correlator multipath rejection for code and carrier," in *10th International Technical Meeting of the Satellite Division of the Institute of Navigation (ION-GPS '97)*, Kansas City, Mo, USA, September 1997, pp. 559–568.

[8] B. R. Townsend, P. C. Fenton, K. J. V. Dierendonck, and D. J. R. van Nee, "Ll carrier phase multipath error reduction using medll technology," in *8th International Technical Meeting of the Satellite Division of the Institute of Navigation (ION-GPS '95)*, Palm Springs, California, September, 1995.

[9] J. Betz, "The offset carrier modulation for GPS

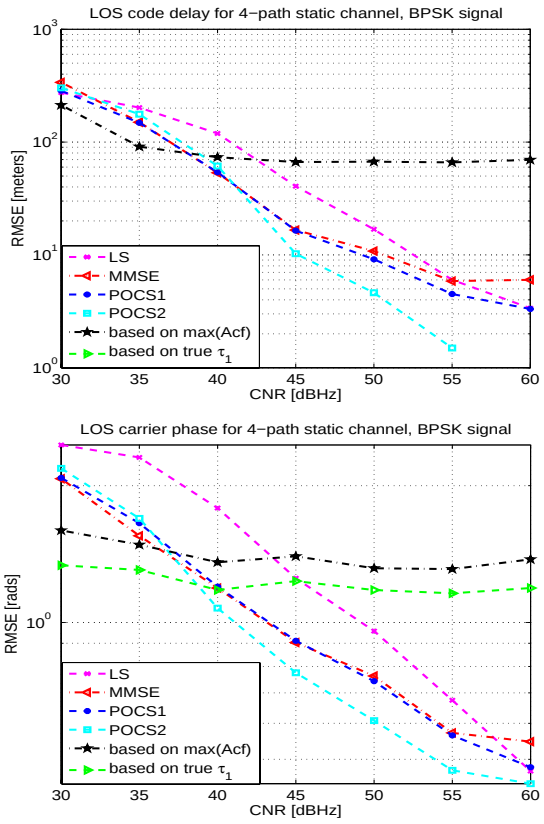


**Fig. 7**. RMSE of LOS code delay and carrier phase offset vs. CNR for 4-path static channel.

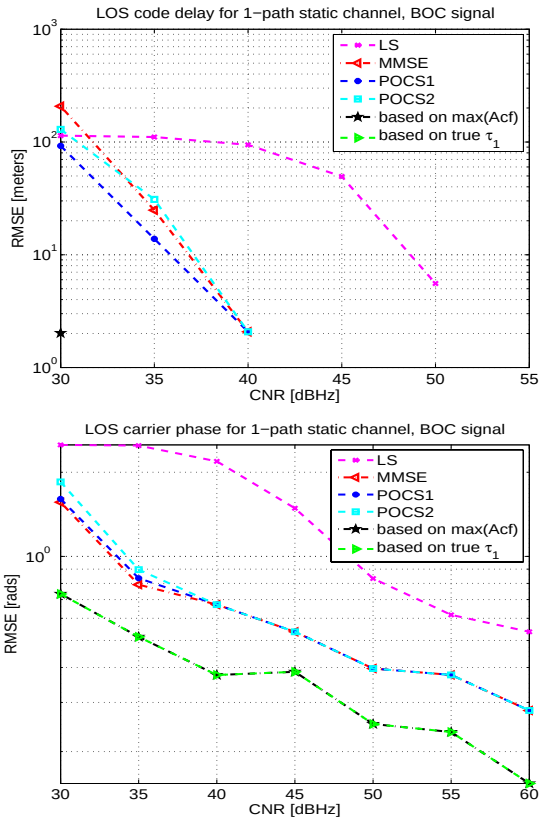


**Fig. 8**. RMSE of LOS code delay and carrier phase offset vs. CNR for 1-path static channel.


modernization," in *Proc. of ION Technical meeting*, 1999, pp. 639–648.

[10] C. J. Hegarty, "Evaluation of the proposed signal structure for the new civil GPS signal at 1176.45 MHz," The MITRE Corporation, Tech. Rep. WN99W0000034, June 1999.

[11] T. Pany, M. Irsigler, B. Eissfeller, and J. Winkel, "Code and carrier phase tracking performance of a future Galileo RTK receiver," in *ENC-GNSS 2002*, Copenhagen, May 2002.

[12] E. S. Lohan, A. Lakhzouri, and M. Renfors, "Feedforward delay estimators in adverse multipath propagation for Galileo and modernized GPS signals," *EURASIP Journal on Applied Signal Processing*, vol. 2006, p. 19, 2006, article ID 50971.

[13] Z. Kostic, M. I. Sezan, and E. L. Titlebaum, "Estimation of the parameters of a multipath channel using set-theoretic deconvolution," in *ICASSP*. IEEE Computer Society, 1991, pp. 1449–1452.

[14] Z. Kostic and G. Pavlovic, "Resolving subchip spaced multipath components in CDMA communication systems," *Vehicular Technology Conference, 1993 IEEE 43rd*, pp. 469–472, May 1993.

[15] D. Colclough and E. Titlebaum, "Delay-Doppler POCS for specular multipath," *ICASSP*, pp. IV–3940–IV–3943 vol.4, 2002.

[16] Z. Kostic and G. Pavlovic, *CDMA RAKE receiver with subchip resolution*, US Patent Publication, US5648983, Lucent Technologies, July 1997.

[17] N. R. Yousef, A. H. Sayed, and N. Khajehnouri, "Adaptive subchip multipath resolving for wireless location systems," *EURASIP J. Appl. Signal Process.*, vol. 2006, no. 1, pp. 151–151, Jan.

[18] "Galileo Joint Undertaking - Galileo Open Service, Signal in space interface control document (OS SIS ICD)," GJU webpages, *http://www.galileoju.com/* (active Oct 2006), May 2006.

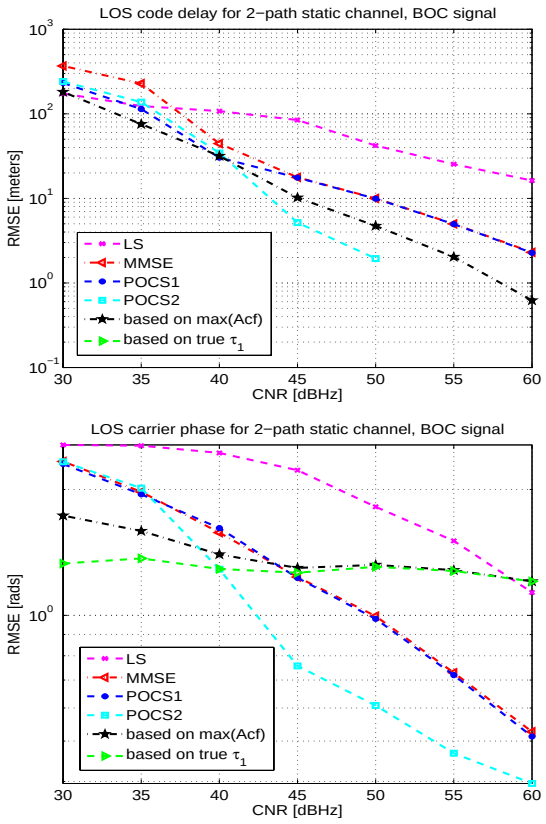


**Fig. 9**. RMSE of LOS code delay and carrier phase offset vs. CNR for 2-path static channel.

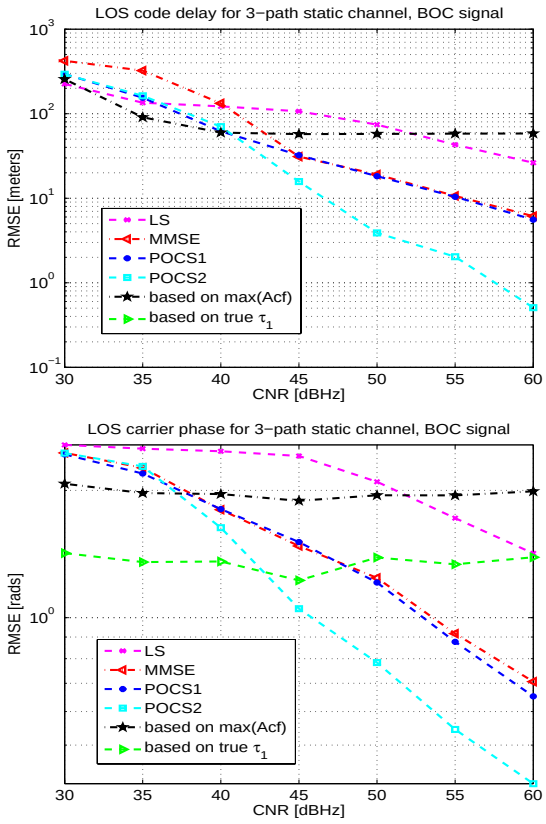


**Fig. 10**. RMSE of LOS code delay and carrier phase offset vs. CNR for 3-path static channel.


[19] G. Hein, J. Avila-Rodriguez, S. Wallner, A. Pratt, J. Owen, J. Issler, J. Betz, C. Hegarty, S. Lenahan, J. Rushanan, A. Kraay, and T. Stansell, "MBOC: The new optimized spreading modulation recommended for Galileo L1 OS and GPS L1C," in *International Technical Meeting of the Institute of Navigation, IEEE/ION PLANS 2006*, San Diego, California, April 2006.

[20] E. S. Lohan, A. Lakhzouri, and M. Renfors, "Binary-offset-carrier modulation techniques with applications in satellite navigation systems," *Wiley Journal of Wireless Communications and Mobile Computing, DOI: 10.1002/wcm.407, published on-line*, July 2006.

[21] A. Lakhzouri, E. S. Lohan, R. Hamila, and M. Renfors, "Extended Kalman filter channel estimation for line-of-sight detection in WCDMA mobile positioning," *EURASIP J. Appl. Signal Processing*, vol. 2003, no. 1, pp. 1268–1278, 2003.

[22] S. Lohan, R. Hamila, and M. Renfors, "Cramer Rao bound for multipath time delays in a DS-CDMA system," in *4th International Symposium on Wireless Personal Multimedia Communications*, Aalborg, Denmark, September 2001, p. 10431046.

[23] D. Skournetou and E. S. Lohan, "Indoor location awareness based on the non-coherent correlation function for GNSS signals," in *Finnish Signal Processing Symposium, FINSIG'07*, Oulu, Finland, August 2007.

[24] ——, "Discontinuity-based code delay estimator for GNSS signals," in *4th Advanced Satellite Mobile Systems (ASMS'08)*, Bologna, Italy, August 2008, in press.

[25] O. Julien, G. Lachapelle, and M. Cannon, "Galileo L1 civil receiver tracking loops' architecture," *Circuits and Systems, 2007. ISCAS 2007. IEEE International Symposium on*, pp. 1737–1741, May 2007.